

# Environmental Science Atmospheres

Volume 6  
Number 3  
March 2026  
Pages 241-452

[rsc.li/esatmospheres](https://rsc.li/esatmospheres)



ISSN 2634-3606



ROYAL SOCIETY  
OF CHEMISTRY

## PAPER

Prince Junior Asilevi, Patrick Boakye *et al.*  
Using pre-monsoon rainwater chemistry to monitor local  
atmospheric pollution in Kumasi, Ghana



Cite this: *Environ. Sci.: Atmos.*, 2026, 6, 273

## Using pre-monsoon rainwater chemistry to monitor local atmospheric pollution in Kumasi, Ghana

Prince Junior Asilevi,<sup>1</sup> Patrick Boakye,<sup>2,3,4,5</sup> Stephen Yaw Owusu,<sup>6</sup> Emmanuel Quansah,<sup>7</sup> Mandela Toku<sup>8</sup> and William Ampomah<sup>9</sup>

Rainwater chemistry offers a valuable tool for atmospheric pollution monitoring in urban environments where air quality is a growing concern. This work evaluated the composition of rainwater in Kumasi, Ghana, during the pre-monsoon season (February to April 2024), focusing on key ions such as  $\text{SO}_4^{2-}$ ,  $\text{NO}_3^-$ ,  $\text{NH}_4^+$ , and  $\text{Cl}^-$ . Rainwater samples were collected from Sokoban (a peri-urban area with localized industrial activities) and KNUST (an urban area) and analyzed for ionic composition. Enrichment factors (EFs) and neutralization factors (NFs) were used to determine pollutant sources (marine, crustal, or anthropogenic) and to evaluate the acid-neutralizing capacity of the rainwater. The results support a conglomerate influence of seasonal dust and anthropogenic activities relating to vehicular emissions and biomass burning, with high nitrate ( $\text{NO}_3^-$ ) concentrations. Local meteorology correlated variably with ion concentrations, with rainfall showing a strong negative correlation with pH ( $r = -0.97/-0.58$ ) indicative of acidification. Maximum temperatures correlated positively with conductivity and turbidity, suggesting enhanced ion concentrations *via* evaporation under warmer conditions. Wind speed enhanced aerosol resuspension, while solar radiation correlated with higher nitrate concentrations, indicating enhanced photochemical reactions. The results highlight a rainwater chemistry-inspired framework to develop guidelines for urban air quality management.

Received 23rd June 2025  
 Accepted 7th December 2025

DOI: 10.1039/d5ea00071h

[rsc.li/esatmospheres](http://rsc.li/esatmospheres)

### Environmental significance

Monitoring atmospheric pollution in rapidly urbanizing regions is crucial for understanding and mitigating air quality issues that impact human health and the environment. This work leverages rainwater chemistry as a cost-effective and insightful tool to assess the sources and dynamics of atmospheric pollutants during the pre-monsoon season in Kumasi, Ghana. By analyzing the ionic composition of rainwater, the work identifies the contributions of local anthropogenic activities, such as vehicular emissions and biomass burning, along with natural sources such as seasonal dust. The study reveals meteorological drivers on pollutant concentrations, offering a nuanced understanding of the interplay between weather conditions and atmospheric chemistry. The findings provide a scientific basis for developing targeted air quality management strategies and policies in urban settings where traditional air quality monitoring infrastructure may be lacking.

## 1. Introduction

Rainwater chemistry holds a unique lens to probe atmospheric pollution dynamics for public health and environmental

management. The composition of rainwater, particularly ionic concentrations such as sulfates ( $\text{SO}_4^{2-}$ ), nitrates ( $\text{NO}_3^-$ ), ammonium ( $\text{NH}_4^+$ ), and chlorides ( $\text{Cl}^-$ ), reflects the influence of natural sources, such as dust and sea salts, and anthropogenic activities such as industrial emissions and biomass burning.<sup>1,2</sup> These chemical markers are key indicators of air quality, environmental risks, cloud condensation nuclei (CCN) in mesoscale convective systems (MCS), and biogeochemical cycles in atmosphere–biosphere systems.<sup>3</sup> Nowadays, air pollution has emerged as a subject of great concern for urban dwellers, and thus rainwater chemistry offers a tool-in-hand to develop air quality guidelines.<sup>1</sup> The West African monsoon system characterized by the oscillatory migration of the Intertropical Convergence Zone (ITCZ), creating distinct dry Harmattan winds laden with Saharan dust followed by summer monsoon

<sup>1</sup>Department of Meteorology and Climate Science, Kwame Nkrumah University of Science and Technology (KNUST), Kumasi, Ghana. E-mail: [pjasilevi@knust.edu.gh](mailto:pjasilevi@knust.edu.gh)

<sup>2</sup>The Brew-Hammond Energy Centre, Kwame Nkrumah University of Science and Technology, Kumasi, Ghana. E-mail: [patrickboakye@knust.edu.gh](mailto:patrickboakye@knust.edu.gh)

<sup>3</sup>Department of Chemical Engineering, Kwame Nkrumah University of Science and Technology, Kumasi, Ghana

<sup>4</sup>Department of Chemistry, Missouri University of Science and Technology, Rolla, MO, USA

<sup>5</sup>Science Laboratory Technology Department, Accra Technical University, Accra, Ghana

<sup>6</sup>Regional Water and Environmental Sanitation Centre Kumasi Laboratories, Kwame Nkrumah University of Science and Technology, Kumasi, Ghana

<sup>7</sup>New Mexico Tech, Petroleum Recovery and Research Center, Socorro, NM 87801, USA



rains, presents a unique opportunity to assess the atmospheric loading of pollutants.<sup>3,4</sup>

Worldwide, rainwater chemistry has been applied as an integrative diagnostic tool. Studies across Asia have demonstrated strong monsoon-driven variability in nitrate, sulfate, and ammonium concentrations, often linked to biomass burning and industrial emissions.<sup>5,6</sup> Across Europe, precipitation chemistry has revealed signatures of traffic emissions, transboundary pollution, and Saharan dust intrusions.<sup>7,8</sup> South American studies similarly show the influence of Amazon biomass burning and industrial aerosols on rainwater composition.<sup>9</sup> Other wet deposition studies highlight interactions between marine aerosols, crustal dust, and anthropogenic sources.<sup>10</sup> Ion composition in rainwater has been used to track industrial emissions, traffic pollution, and agricultural activities.<sup>11,12</sup> For example, Zeng *et al.* established that urban contributions from coal combustion, industry, traffic, and agriculture resulted in 93% of  $\text{NO}_3^-$ , 62% of  $\text{SO}_4^{2-}$ , and 87% of  $\text{NH}_4^+$  in rainwater samples collected in the Maolan National Karst Forest Park. They also identified key sources contributing to  $\text{NO}_3^-$  and  $\text{SO}_4^{2-}$  in rainwater in Beijing.<sup>13</sup> These examples reinforce the versatility of rainwater chemistry in capturing gaseous pollutants, particulate matter, and aerosols, and in diagnosing atmospheric processes across climates.<sup>11,12</sup>

In West Africa (WA), the interaction between natural dust (predominantly from the Sahara) and anthropogenic pollutants presents unique challenges for air quality management. The Harmattan season is marked by high dust concentrations that degrade visibility and exacerbate pollution levels.<sup>14</sup> Studies in the region have highlighted the role of dust in shaping rainwater chemistry.<sup>15,16</sup> However, atmospheric interactions during transitional seasons remain insufficiently explored, especially under a warming climate and rapidly urbanizing environments. Similar dust–pollution interactions have been extensively documented in Asia, the Arabian Peninsula, and Australia, where large-scale dust storms significantly influence wet deposition acidity and crustal ion dominance.<sup>17,18</sup> Over the WA region, however, the Saharan dust transport intensity and seasonality present a globally unique environment.

Despite the growing concern over urban air quality in West Africa, the chemical composition of rainwater during the transitional pre-monsoon period remains nascent. Kumasi, Ghana's second-largest city, with its mosaic of urban and peri-urban microenvironments, represents a critical site for evaluating wet deposition chemistry in a tropical setting. Comparable transitional-season analyses in South Asia and South America have shown that early-season rainfall often contains some of the highest ionic concentrations of the year due to prolonged pollutant accumulation during dry months.<sup>19</sup> Such events provide critical insight into atmospheric cleansing mechanisms prior to sustained monsoon rainfall. The primary aim of this study is to explore the utility of pre-monsoon rainwater chemistry as a tool for monitoring atmospheric pollution. Specifically, the study seeks to characterize the ionic composition of rainwater (*e.g.*,  $\text{SO}_4^{2-}$ ,  $\text{NO}_3^-$ ,  $\text{NH}_4^+$ ,  $\text{Cl}^-$ ,  $\text{Ca}^{2+}$ , and  $\text{Mg}^{2+}$ ) collected from two contrasting locations in Kumasi; investigate spatial differences and temporal variability in physicochemical

properties of rainwater; analyze the influence of meteorological factors such as rainfall, temperature, humidity, and wind on ionic concentrations; and identify dominant pollution sources *via* enrichment factor (EF), neutralization factor (NF), and air mass trajectory analysis. The objectives respond to the need for low-cost, scalable approaches to air quality surveillance and provide baseline data for future long-term monitoring efforts. This work is exploratory due to the limited number of rainfall events during the pre-monsoon season and the absence of prior rainwater chemistry monitoring in Kumasi. It is intended as a baseline assessment to inform future long-term and multi-season studies in the region.

## 2. Materials and methods

### 2.1. Geography and climate of the study area

Greater Kumasi (6.7° N, 1.6° W), located in Ghana's forest zone, experiences a tropical wet and dry climate. The study was conducted at two sites within the city (see Fig. 1): Sokoban and the Regional Water and Environmental Sanitation Center Kumasi (RWESCK) at the Kwame Nkrumah University of Science and Technology (KNUST). Kumasi, known as the “Garden City of West Africa”, was designed following the Howard Garden City Model, though urbanization has reduced its vegetative cover (~25 km<sup>2</sup>) significantly in recent years.<sup>20,21</sup> Sokoban is a peri-urban area characterized by industrial activities such as wood processing, sawdust burning, charcoal production, and animal hide roasting, contributing to smoke and dust emissions. In contrast, RWESCK-KNUST, approximately 17 km away, represents an urban hub influenced by vehicular emissions, biomass burning, and natural dust from the Harmattan winds.

Kumasi has distinct wet and dry seasons, with the pre-monsoon period (February to April) marking the transition to the West African monsoon. This period is dominated by dry Harmattan winds, which carry Saharan dust, impacting air quality and atmospheric chemistry. The city's rainfall is bimodal, peaking in May–June and September–October, while pre-monsoon temperatures range from 17 °C to 36 °C.<sup>22,23</sup>

### 2.2. Rainwater sampler equipment

Rainwater samples were collected at the designated sites during the dry-to-wet transitional pre-monsoon season between February and April 2024. A specialized homemade Atmospheric Wet Deposition Rainwater Sampler (ARS), shown in Fig. 2, was designed to carry out the sampling. A collection funnel (13 cm in diameter) channels rainwater into a secure sample container, together making 51 cm in height. The system stands tall at 150 cm, mounted on sturdy legs designed to provide stability and elevation, minimizing ground contamination and splashing effects. At the core, a bulkhead fitting ensures a seamless flow from the funnel to an internal sample bottle. To prevent dry dust deposition before rain, the sampler was equipped with a protective lid that covered the collection funnel during non-rain periods. The lid was removed just before the onset of rainfall, and the sampler was promptly retrieved after the rain event concluded. This ensured minimal contamination from



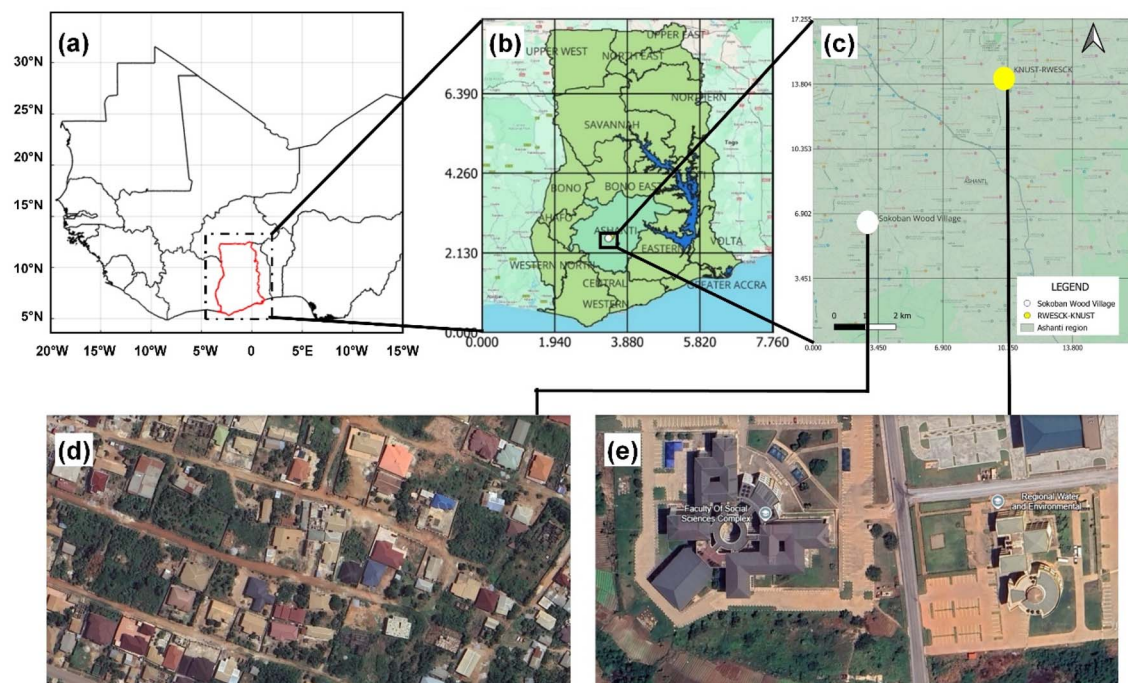


Fig. 1 Location of the study area showing (a) the West African region, (b) Ghana within the WA region, (c) the city of Kumasi, (d) and (e) the two sampling sites (Sokoban and RWESCK-KNUST).

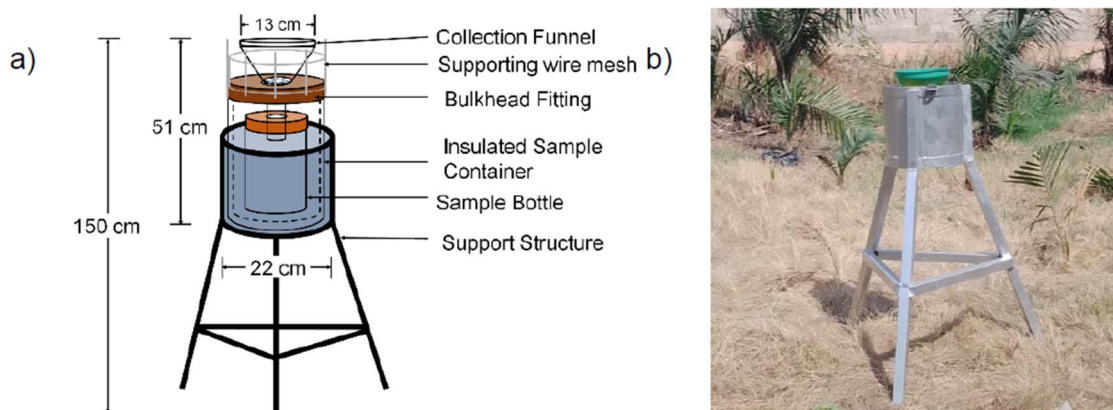


Fig. 2 (a) A 3D schematic design of the rainwater sampler and (b) mounted rainwater sampler at the Sokoban wood village in Kumasi, Ghana.

dry atmospheric fallout and safeguarded the integrity of the samples. Generally, the design followed established guidelines for the World Meteorological Organization Global Atmosphere Watch (WMO-GAW) Precipitation Chemistry Programme<sup>26</sup> and is similar to wet-deposition collectors widely used in atmospheric chemistry studies.<sup>15,16</sup>

Most significant rains in the pre-monsoon period are short-lived, heavy downpours. Following the WMO-GAW Precipitation Chemistry Program, rainwater samples were collected immediately after the rain episodes concluded to ensure representative washout effects. For midnight rainfall events, samples were retrieved just before sunrise.<sup>26</sup>

Recent thirty (30) years of climatological data show that rainfall in Kumasi commences in the neighborhood of the

second week of March (*i.e.* around Julian day 70). During this period, a steady rise in mean precipitation, wind speeds, temperature, and consequently relative humidity is recorded. The winds are highly variable due to the recessing dust-laden continental trade winds and oncoming maritime winds conveyed by the Intertropical Convergence Zone (ITCZ). Thus to achieve accurate chemical representation of this period, the field scheme was designed to ensure collection of the very first rainfall for the year 2024 at the sites of interest until the climatological onset. The pre-monsoon rains have resulted from a combination of factors including the northward migration of the ITCZ, pre-monsoon depressions, local convection due to variable land heating, and variations in outgoing long-wave radiation.<sup>25,26</sup>



### 2.3. Chemical assessment and analytical methods

**2.3.1. Sample analysis.** The pH and conductivity of the rainwater samples were measured immediately after sampling using a multiparameter pH analyzer (Hach, HQ440d). The samples were filtered, and turbidity was measured using a Hach 2100Q Portable Turbidimeter. They were then stored under refrigeration to minimize potential physicochemical changes before laboratory analysis. Subsequently, the samples were analyzed for  $\text{NH}_4^+$  (Nessler Reagent).  $\text{SO}_4^{2-}$  and  $\text{NO}_3^-$  were also measured using a HachDr6000 Spectrophotometer with PER-MACHEM Reagent, respectively, while  $\text{Ca}^{2+}$ ,  $\text{Na}^+$ ,  $\text{Mg}^{2+}$ ,  $\text{K}^+$  and  $\text{Cl}^-$  were analyzed by titrimetry.

The laboratory data for each sample analysis were quality-controlled by the ion balance technique. The  $1 \pm 0.25$  criteria for the total anions to cations ratio (A/C) showed a few imbalances. The mean A/C ratios for all samples were 0.41 and 0.50 for Sokoban and RWESCK-KNUST respectively, with a few lower A/C values than the quality criteria, indicative of significant cation dominance, likely due to unmeasured  $\text{HCO}_3^-$ . The concentration of  $\text{HCO}_3^-$  was thus estimated following eqn (1) recommended by the World Meteorological Organization Global Atmosphere Watch Precipitation Chemistry Programme to ensure A/C quality.<sup>24</sup>

$$[\text{HCO}_3^-] = \frac{5.1}{10^{9-\text{pH}}} \quad (\text{for } \text{pH} > 5.0) \quad (1)$$

Thereafter, new mean A/C values of 0.90 for Sokoban and 1.2 for RWESCK-KNUST are realized, though some samples still fell below the quality threshold. This could reflect the seasonality of the pre-monsoon period, during which Saharan dust and open burning contribute to elevated cation concentrations in rainwater, affecting the ion balance.<sup>27</sup>

Advanced methods such as ion chromatography and ICP-MS are recommended in future studies to improve detection accuracy and expand chemical resolution.

**2.3.2. Enrichment Factor (EF).** The Enrichment Factor (EF) was used to determine the relative contribution of natural sources (*e.g.* sea salt and crustal dust) and anthropogenic activities to the ionic composition of rainwater. The EF calculation allows for distinguishing between ions originating from natural processes and those enriched by human activities, such as industrial emissions, vehicular exhaust, and biomass burning. For the marine source contribution, sodium ( $\text{Na}^+$ ) was used as a reference element, being a major constituent of sea salt. For crustal sources, calcium ( $\text{Ca}^{2+}$ ) was used as the reference due to its abundance in soil and crustal material. The EF for marine and crustal sources was calculated using the following equations:

$$\text{EF}_{\text{marine}} = \frac{(X/\text{Na}^+)_{\text{rainwater}}}{(X/\text{Na}^+)_{\text{seawater}}} \quad (2)$$

$$\text{EF}_{\text{crustal}} = \frac{(X/\text{Ca}^+)_{\text{rainwater}}}{(X/\text{Ca}^+)_{\text{crust}}} \quad (3)$$

where  $X$  is the concentration of the ion of interest,  $(X/\text{Na}^+)_{\text{seawater}}$  and  $(X/\text{Ca}^+)_{\text{crust}}$  are typical seawater and crustal ratios.<sup>28</sup> EF values greater than 1 indicate an excess of the ion in rainwater relative to natural sources, suggesting an anthropogenic contribution. Conversely, EF values close to 1 suggest that the ion is predominantly derived from natural sources, such as sea salt or crustal material.

**2.3.3. Neutralizing Factor (NF).** The Neutralizing Factor (NF) is used to evaluate the capacity of alkaline species in rainwater to neutralize acidic components, such as sulfates ( $\text{SO}_4^{2-}$ ) and nitrates ( $\text{NO}_3^-$ ), which are associated with acid rain. The presence of cations such as calcium ( $\text{Ca}^{2+}$ ), magnesium ( $\text{Mg}^{2+}$ ), ammonium ( $\text{NH}_4^+$ ), and potassium ( $\text{K}^+$ ) can mitigate the acidity of rainwater by neutralizing strong acids. The NF for each major alkaline ion was calculated as follows:

$$\text{NF}_X = \frac{[X]}{[\text{SO}_4^{2-}] + [\text{NO}_3^-]} \quad (4)$$

where  $X$  represents the concentration of the alkaline ion ( $\text{Ca}^{2+}$ ,  $\text{Mg}^{2+}$ ,  $\text{NH}_4^+$ , or  $\text{K}^+$ ).  $[\text{SO}_4^{2-}]$  and  $[\text{NO}_3^-]$  represent the total concentrations of acidic anions. The NF evaluates the buffering capacity of rainwater against acidification.<sup>28</sup>

### 2.4. Meteorological data

An integrated station- and satellite-based reanalysis meteorological dataset spanning the sampling period *i.e.* 1st January to 31st April 2024 was obtained from a nearby Ghana Meteorological Agency Synoptic weather station and NASA's Prediction of Worldwide Energy Resources (POWER) retrieved at <https://power.larc.nasa.gov/data-access-viewer/>. The dataset comprised daily rainfall, temperature, relative humidity, wind speed, and solar irradiance to achieve an all-round evaluation. The integration served the advantage of augmenting station measurement with unavailable data such as the all-sky solar irradiance as well as ensuring a distributed representation of the local meteorology, considering that the collection sites are  $\sim 10$  km away from the weather station. NASA POWER is a 0.5-degree area gridded global dataset, which has been extensively validated over the region and shown to be a good representation of local climatology.<sup>29–32</sup>

## 3. Results and discussion

### 3.1. Pre-monsoon micrometeorology and weather dynamics

A key focus of this work is the micrometeorological drivers of rainwater chemistry. Fig. 3 presents the daily mean meteorological data over Kumasi from 1st January to 30th April 2024, focusing on key weather parameters, including rainfall, temperature, relative humidity (RH), and wind speeds at 2 meters (Wind2M) and 10 m (Wind10M). Fig. 3a indicates a predominantly dry period, with scattered rainfall events reaching  $35.9 \pm 6.2$  mm between March and April. This coincides with temperature fluctuations, which remain relatively stable, though a slight increase is observed as the pre-monsoon transitions into the onset of the wet season. Rainwater during the early rainfall events tends to capture higher concentrations



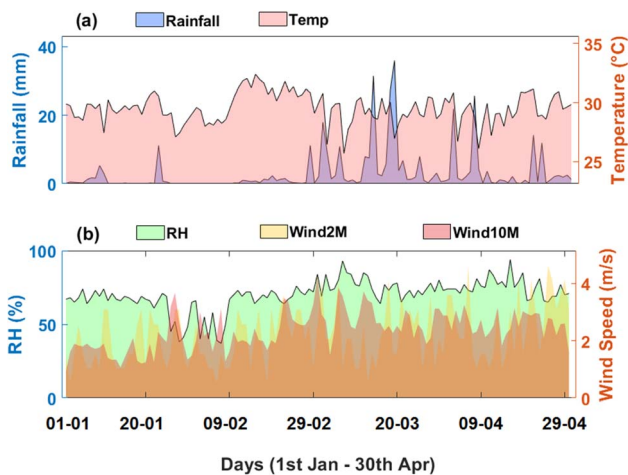


Fig. 3 Daily meteorological conditions over Kumasi, Ghana, from 1st January to 30th April 2024 for (a) daily rainfall (mm) and air temperature ( $^{\circ}\text{C}$ ), and (b) daily mean relative humidity (%), and wind speed at 2 m and 10 m height.

of pollutants that have accumulated in the atmosphere during the dry season. The washout effect, where rain scavenges airborne particles and gases, is expected to be more pronounced during this period.

The relative humidity in Fig. 3b shows an upward trend, reflecting the gradual transition from dry Harmattan conditions to wetter monsoon influences. Notable peaks in RH align with rainfall events, as increased atmospheric moisture follows precipitation. In contrast, wind speeds, especially at 10 m, exhibit considerable variability, with stronger gusts recorded in March and April, potentially related to the influence of Harmattan winds. These dry, dust-laden winds are significant drivers of air quality deterioration, transporting fine dust particles across the region. Higher wind speeds can enhance the transport of dust and pollutants, impacting the composition of rainwater during precipitation. The vertical gradient observed between Wind2M and Wind10M suggests stratification, where pollutants are differentially dispersed at different altitudes. This stratification could affect the chemical composition of rainwater collected, with stronger winds likely contributing to higher dust and particulate deposition in rainwater samples.

The dry winds, characterized by high dust loads, combined with low rainfall, contribute to a buildup of atmospheric pollutants. The onset of the first rains likely serves to cleanse the atmosphere, capturing both natural and anthropogenic pollutants. This study leverages the unique meteorological conditions during the pre-monsoon season to evaluate rainwater as a tool for air quality monitoring. Specifically, the data provides an opportunity to trace the influence of meteorological drivers on the chemical composition of rainwater.

The pre-monsoon period preceding the main rains in March is characterized by a dry season with minimal rainfall. During this period, only sporadic rainfall events occurred, many of which produced insufficient volumes (below 50 mL) for meaningful chemical analysis. Consequently, the dataset for this study comprised 10 precipitation samples (5 from each site),

Table 1 Physical parameters of rainwater samples at Sokoban

Date	pH	EC ( $\mu\text{S cm}^{-1}$ )	Turbidity (NTU)
20th Feb	6.30	100	55.1
3rd Mar	6.34	27.2	14.2
5th Mar	6.89	31.1	66.8
7th Mar	6.54	18.5	5.0
15th Mar	6.47	50.3	12.6

representing the best possible collection under these challenging conditions. While this limits the scope of conclusions drawn, the findings serve as valuable baseline data for understanding rainwater chemistry in this transitional period.

### 3.2. Rainwater physicochemical composition and trend

Fig. 4 illustrates the trends in dissolved ions at Sokoban and RWESCK-KNUST. At Sokoban (Fig. 4a), nitrate ( $\text{NO}_3^-$ ) concentrations dominate initially, reaching  $12 \text{ mg L}^{-1}$ , indicative of intense pollution, likely from biomass burning and industrial emissions. This is followed by a sharp decline, reflecting the washout effect due to early rainfall events. Ammonium ( $\text{NH}_4^+$ ) concentrations also exhibit temporal fluctuations, with elevated levels pointing to agricultural emissions. At RWESCK-KNUST (Fig. 4b), nitrate concentrations again dominate, peaking at  $10 \text{ mg L}^{-1}$ , particularly during the late March rainfall. This suggests a similar source of nitrogenous pollutants from urban traffic and industrial activities. The consistently high levels of calcium ( $\text{Ca}^{2+}$ ) at both sites are indicative of crustal dust contributions, likely from the Harmattan dust, combined with local pollution sources. Both locations demonstrate an inverse relationship between rainfall volume and ion concentrations, underscoring the scavenging effect of rain on atmospheric pollutants. The data reveal that rainfall intensity significantly influences the temporal dynamics of ion concentrations.<sup>33</sup>

It is worth noting that, while Sokoban features pockets of industrial and manufacturing activities such as wood processing, sawdust burning, and small-scale manufacturing, these activities are not as intense as those found in larger cities such as Accra. However, their localized nature still contributes significantly to the area's air quality, particularly in comparison to KNUST.

Fig. 4c and d depict the percentage composition of dissolved ions at Sokoban and RWESCK-KNUST, respectively. At Sokoban, the ionic composition is dominated by  $\text{Ca}^{2+}$  (26%) and  $\text{NO}_3^-$

Table 2 Physical parameters of rainwater samples at RWESCK-KNUST

Date	pH	EC ( $\mu\text{S cm}^{-1}$ )	Turbidity (NTU)
29th Feb	6.73	1850	79.3
3rd Mar	6.58	73.0	20.8
7th Mar	6.94	44.5	10.4
15th Mar	6.43	33.7	20.7
3rd Apr	6.13	56.4	11.6



(25%), reflecting significant contributions from dust storms, biomass burning, and vehicular emissions. The presence of  $Mg^{2+}$  (20%) and  $SO_4^{2-}$  (2%) indicates a mix of natural dust and secondary anthropogenic sources. At RWESCK-KNUST, the ionic profile shows a similar dominance of  $Ca^{2+}$  (24%) and  $NO_3^-$  (25%). However,  $Ca^{2+}$  (24%) and  $Mg^{2+}$  (22%) make up a substantial portion of the composition, suggesting a more pronounced crustal and natural dust contribution at this urban site. The relatively lower contribution of  $SO_4^{2-}$  across both sites suggests limited influence of fossil fuel combustion or industrial sulfur emissions. The observed ionic composition similarity at both sites suggests a dominant influence of regional sources such as Saharan dust and biomass burning, which affect the entire Kumasi area. However, turbidity and electrical conductivity differences may reflect localized influences, including industrial wood processing and charcoal burning at Sokoban, and road-related emissions and construction near KNUST.

Table 1 and 2 summarize the physical parameters of the rainwater samples. The pH values at both sites indicate slightly acidic to near-neutral rainwater, with Sokoban showing a more alkaline trend in the 5th March sample (pH 6.89), possibly due to the influence of local anthropogenic activities such as biomass burning and industrial emissions. The electrical conductivity (EC) values fluctuate significantly, particularly at RWESCK-KNUST, where an abnormally high EC value of  $1850 \mu S cm^{-1}$  was recorded on 29th February. This could reflect heavy contamination, potentially from local vehicular emissions, as the sampling site is near an ongoing road construction site.

Turbidity levels vary widely between samples at both sites, with Sokoban showing a peak turbidity of 66.75 NTU on 5th March, which might indicate increased particulate matter deposition, likely from nearby wood processing or waste burning activities. Similarly, RWESCK-KNUST exhibits high turbidity levels, particularly on 29th February (79.3 NTU), which

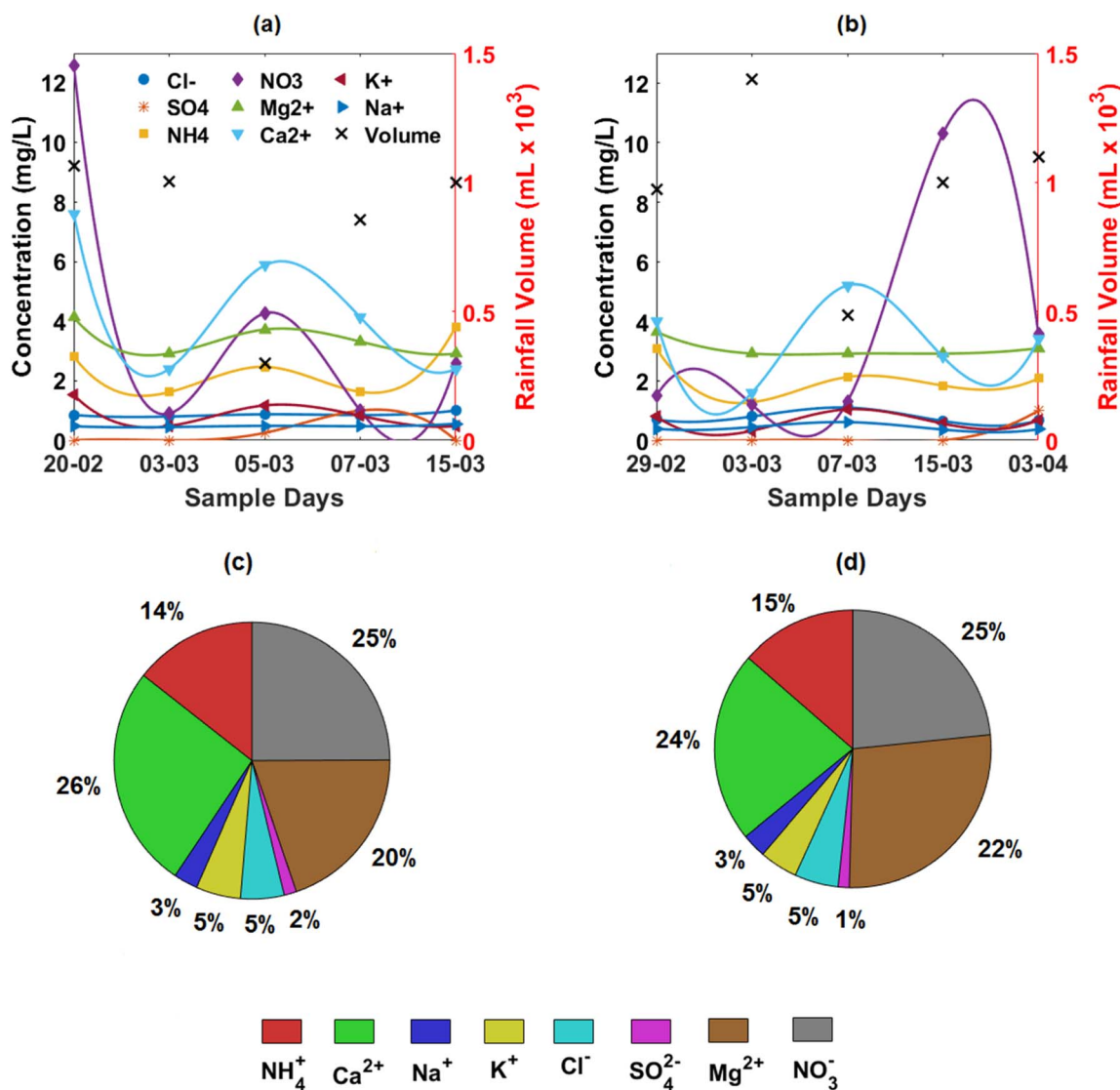


Fig. 4 Temporal trends and percentage composition of dissolved ionic species in 2024 pre-monsoon rainwater collected at (a–c) Sokoban and (b–d) RWESCK-KNUST, Kumasi, Ghana. (a) and (b) show ion concentration variability ( $mg L^{-1}$ ). (c) and (d) show the relative (%) contribution of each ion.



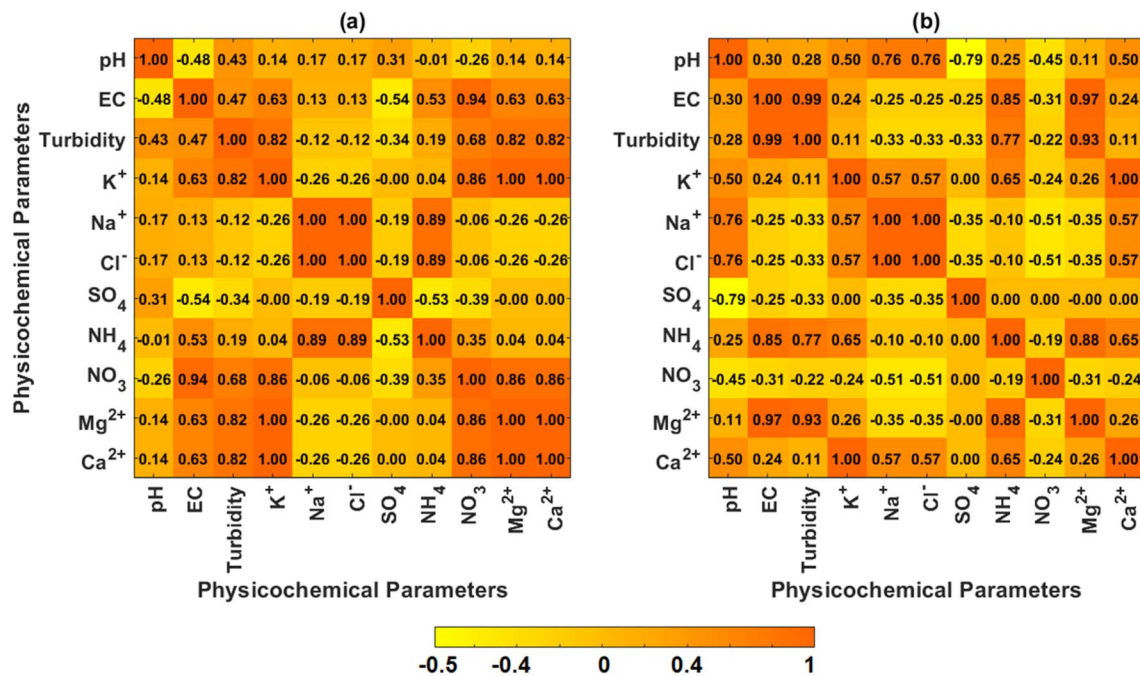


Fig. 5 Correlation matrices of rainwater physicochemical parameters and ionic species for samples collected in 2024 at (a) Sokoban and (b) RWESCK-KNUST, Kumasi, Ghana. Positive and negative correlations illustrate site-specific pollutant interactions.

aligns with the high EC value, suggestive of a period of significant atmospheric particle loading, possibly from a conglomerate of dust surges, emissions, and local construction.

At Sokoban (Fig. 5a), EC and turbidity exhibit a fairly positive correlation (0.47), suggesting that dissolved ions increase with suspended particulates. This is likely due to the influence of local pollution sources such as biomass burning and sawdust-related activities. Notably, NO<sub>3</sub><sup>-</sup> and NH<sub>4</sub><sup>+</sup> show a weak positive correlation (0.35), reflecting the independent contribution of their sources. Furthermore, K<sup>+</sup> exhibits a perfect positive correlation with Ca<sup>2+</sup>, which can be attributed to contributions from biomass burning or crustal dust.

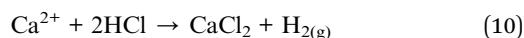
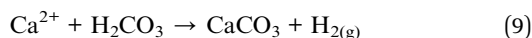
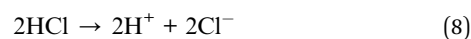
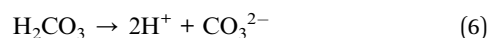
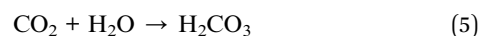
At RWESCK-KNUST (Fig. 5b), turbidity has a weak correlation with pH (0.25) and Ca<sup>2+</sup> (0.11), indicating that suspended particulates are not well associated with dust particles and other crustal materials. SO<sub>4</sub><sup>2-</sup> and NO<sub>3</sub><sup>-</sup> are not correlated, suggesting differing atmospheric processes governing their presence in rainwater. The presence of NO<sub>3</sub><sup>-</sup>, a key indicator of anthropogenic pollution, likely results from vehicular emissions, whereas SO<sub>4</sub><sup>2-</sup> contributions may come from both natural and anthropogenic sources, including dust transport and industrial activities.

### 3.3. Possible sources of the physicochemical composition of the pre-monsoon rains

Rainwater EC values below 10 μS cm<sup>-1</sup> are usually considered normal.<sup>34</sup> The EC values obtained here are higher than normal. This indicates the presence of several dissolved ions in the rain. However, the EC values in this study decreased with time, which suggests that the concentration of salts (KCl, NaCl, MgCl<sub>2</sub>, CaCl<sub>2</sub> and the nitrate salts) in the rainwater decreased as the

rains gradually transitioned from the pre-monsoon to the actual monsoon season. This further accentuates the potential of pre-monsoon rains for air pollution monitoring. Also, the first collection of rainwater samples was very turbid. This results from the existence of more suspended dust particles due to atmospheric pollution. The turbidity reduced with time as more rains fell to remove suspended particles and bring clarity to the atmosphere.

The pH of normal rainwater is ~5.5, which is slightly acidic. This is due to the dissolution of atmospheric CO<sub>2</sub> with water to form carbonic acid (eqn (5)), which further dissociates into H<sup>+</sup> ions as shown in eqn (6). CO<sub>2</sub> is abundant in the atmosphere due to the use and burning of fossil fuels.<sup>35</sup> NaCl from sea salt also reacts with H<sub>2</sub>SO<sub>4</sub> present in the atmosphere to form sodium sulfate and hydrogen chloride (eqn (7)), which also contributes to the acidic value of rainwater through dissociation into H<sup>+</sup> ions (eqn (8)). In this study, however, the pH of the pre-monsoon rainwater collected was ~7, which is almost neutral. This suggests that the rainwater also contain other pollutants such as calcium ions from calcium carbonate, which causes the neutralization reactions (eqn (9) and 10).



Calcium carbonate, generally from dust, is indicative of atmospheric dust pollution in rainwater. Dust can also contain other elements such as sulfur, chlorine, nitrogen, potassium, sodium, magnesium and heavy metals. Potassium ions can be discharged into the atmosphere through dust and biomass burning while calcium ions are primarily dissolved in rainwater through weathering of rocks such as limestone and dolomite. Since Fig. 4 shows that the percent of  $\text{Ca}^{2+}$  (26%) is greater than that of  $\text{K}^+$  ions (5%) in the pre-monsoon water samples collected, it suggests that calcium ions contribute significantly to the neutralization of the rainwater compared to potassium ions.<sup>36</sup>  $\text{NH}_4^+$  ions in the pre-monsoon rainwater samples originate primarily from the dissolution of ammonia with water in the atmosphere. Atmospheric ammonia is also often contributed by agricultural activities such as fertilizer use and livestock waste or can be obtained from particulate matter in the air. The high percentage of magnesium ions observed in the rainwater is obtained from dissolved minerals from dust collected from the Earth's crust.<sup>37</sup> This high concentration of magnesium ions is not unusual, since Kumasi is close to Obuasi (60 km apart), where there is huge mining of minerals.

Chloride ions predominantly originate from sea salt aerosols and therefore their concentration increases in rainwater closer to an ocean compared to dry land.<sup>38</sup> Since Kumasi is not near the Atlantic Ocean, percentage of chloride ions is expected to be negligible. The small percentage (5%) of chloride ions in the pre-monsoon water samples collected can therefore be attributed to the transportation of chloride ions in aerosols to the inland by winds. Sulphate ions (1%) dissolved in water is primarily from the oxidation of sulfur dioxide, which is emitted during the combustion of fossil fuels, due to the release of sulfur compounds. Sulfur compounds are naturally abundant in volcanic areas,<sup>39</sup> and since Kumasi is not a volcanic area, this

probably explains the low percentage of sulfur ions in the pre-monsoon rainwater samples collected. The primary source of atmospheric nitrogen oxides is from burning biomass and fossil fuel. Since Kumasi is a city with minimal biogenic activities, the high percentage of nitrate ions observed (Fig. 4) can be attributed to the abundance of fossil fuel burning. Since each physicochemical composition of the pre-monsoon rains can be attributed to certain pollution activities, it suggests that pre-monsoon rainwater chemistry can be used as a tool to monitor atmospheric pollution and develop guidelines for air quality management in Kumasi and, by extension, areas across the globe with similar climate conditions.

### 3.4. Composition and micrometeorology correlations and impact

The meteorological drivers influencing ionic concentrations are presented in Fig. 6. At Sokoban (Fig. 6a), rainfall has a strong negative correlation with pH ( $r = -0.97$ ), suggesting that higher rainfall events contribute to more acidic rainwater, likely due to increased scavenging of atmospheric pollutants.<sup>33</sup> Rainfall also exhibits a positive correlation with electrical conductivity (EC,  $r = 0.42$ ), indicating that larger rain events capture more atmospheric particulates, while reducing turbidity, reflecting the dilution of suspended particles. Temperature influences ion concentrations significantly. Maximum temperature ( $T_{\text{max}}$ ) positively correlates with EC and turbidity, suggesting that higher temperatures, which promote evaporation, concentrate ions in rainwater. This is also reflected in the positive correlations of  $T_{\text{max}}$  with nitrates ( $\text{NO}_3^-$ ,  $r = 0.66$ ) and ammonium ( $\text{NH}_4^+$ , 0.79), which are often associated with local emissions such as biomass burning. Minimum temperature ( $T_{\text{min}}$ ) shows strong correlations with major ions such as potassium ( $\text{K}^+$ ,  $r = 0.95$ ) and calcium ( $\text{Ca}^{2+}$ ,  $r = 0.95$ ), suggesting the effect of

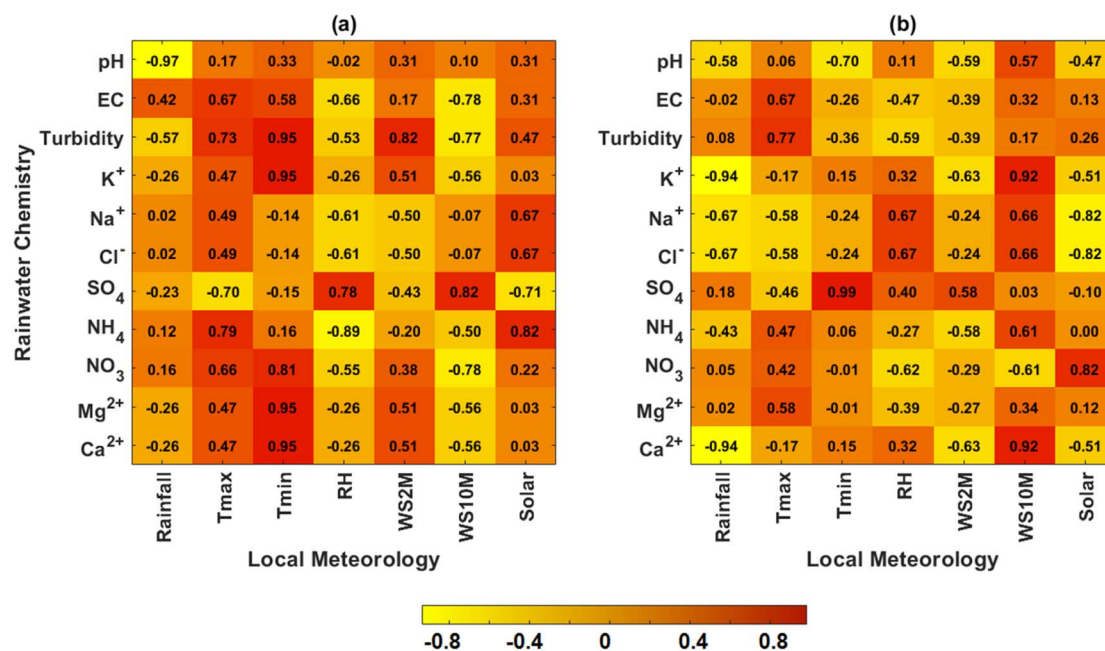


Fig. 6 Correlation matrices of meteorological drivers on atmospheric ions at (a) Sokoban and (b) RWESCK-KNUST.



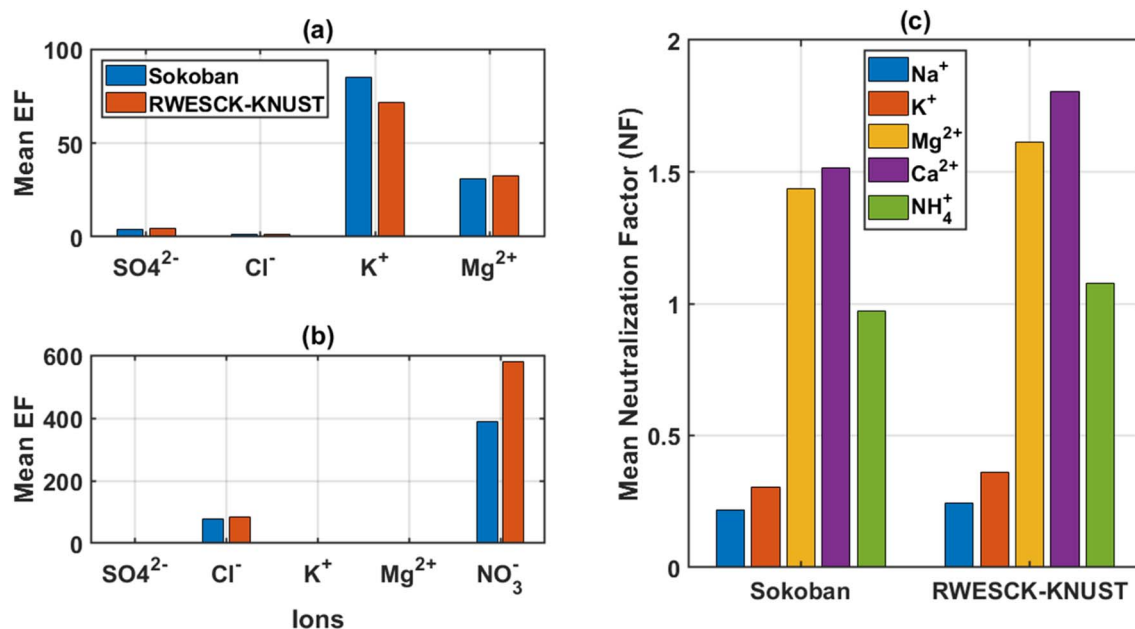


Fig. 7 Comparison of mean enrichment factor (EF) for (a) marine and (b) crustal sources, and (c) neutralization factor (NF).

condensation on dust particles during cooler periods. Relative humidity (RH) generally has negative correlations with most rainwater chemistry parameters, implying that high humidity helps suppress dust and particulate matter, resulting in cleaner rainwater. Wind speeds at both 2 m and 10 m influence particulate concentrations, with higher surface winds increasing turbidity by suspending dust, while stronger winds at 10 m tend to dilute finer pollutants such as nitrates. Solar radiation shows a weak positive correlation with EC, indicative of solar intensity impact on atmospheric ionization *via* photochemical reactions.

At RWESCK-KNUST (Fig. 6b), rainfall shows similar impact on pH by a moderate negative correlation of  $r = -0.58$ , suggestive of acidity due to the washout. The strong negative correlation of rainfall with potassium ( $\text{K}^+$ ,  $r = -0.94$ ), sodium ( $\text{Na}^+$ ,  $r = -0.67$ ), and chloride ( $\text{Cl}^-$ ,  $r = -0.67$ ) implies that higher rainfall events efficiently remove these ions from the atmosphere. Additionally, rainfall has a moderate negative correlation with ammonium ( $\text{NH}_4^+$ ,  $r = -0.43$ ) and calcium ( $\text{Ca}^{2+}$ ,  $r = -0.94$ ), reflecting the scavenging of local pollutants. Maximum temperature positively correlates with electrical conductivity (EC,  $r = -0.67$ ) and turbidity ( $r = -0.77$ ), indicating that warmer conditions enhance the evaporation of water droplets, leading to more concentrated ions in rainwater. Conversely, minimum temperature exhibits negative correlations with pH ( $r = -0.70$ ),  $\text{Na}^+$  ( $r = -0.24$ ), and  $\text{Cl}^-$  ( $r = -0.58$ ), suggesting that cooler conditions likely trap pollutants closer to the ground, enhancing rainwater acidity and salinity. Relative humidity has a generally negative influence on ion concentrations, as seen in its strong negative correlations with nitrates ( $\text{NO}_3^-$ ,  $r = -0.62$ ) and ammonium ( $\text{NH}_4^+$ ,  $r = -0.27$ ), reflecting that higher humidity helps in dispersing or diluting these pollutants in the atmosphere. Wind speeds at 2 m and 10 m show mixed correlations, with higher wind speeds correlating

positively with  $\text{K}^+$  ( $r = -0.92$ ) and  $\text{Ca}^{2+}$  ( $r = -0.92$ ), corroborating the situation of dust and crustal particle resuspension at Sokoban. Solar radiation adds important further detail by the strong positive correlation with nitrates ( $\text{NO}_3^-$ ,  $r = 82$ ), indicating that increased shortwave irradiance enhanced photochemical reactions that produce nitrates.

Overall, the meteorological dynamics at Sokoban and RWESCK-KNUST highlight the complex interplay between rainfall, temperature, wind, and solar radiation in modulating the ionic concentration and transformation in rainwater, pointing to the influence of both local emissions and regional dust transport.

The data on enrichment factors (EF) and neutralization factors (NF) presented in Fig. 7 shed insights into the sources and chemical interactions. For marine sources (Fig. 7a), both locations exhibit relatively low EF values for sulfate ( $\text{SO}_4^{2-}$ ) and chloride ( $\text{Cl}^-$ ), indicating minimal marine influence on these ions. However, potassium ( $\text{K}^+$ ) shows significantly higher enrichment, especially at Sokoban, where anthropogenic sources such as biomass burning and industrial activities are more prominent. Magnesium ( $\text{Mg}^{2+}$ ) also displays moderate enrichment, pointing to a mix of natural crustal and marine inputs. For crustal sources (Fig. 7b), nitrate ( $\text{NO}_3^-$ ) stands out with extremely high enrichment factors at both sites, with RWESCK-KNUST showing a higher EF than Sokoban, suggesting significant contributions from anthropogenic sources such as vehicular emissions and industrial activities (in this case road construction). The high EF for chloride at RWESCK-KNUST further highlights the influence of crustal dust, which is more prominent in this urbanized area. The consistently low EF for potassium and magnesium at both sites suggests that these ions are less affected by crustal sources, aligning more with anthropogenic emissions.



The neutralization factor (NF) computation presented in Fig. 7c illustrates the capacity of different cations to neutralize the acidic components. Calcium ( $\text{Ca}^{2+}$ ) and magnesium ( $\text{Mg}^{2+}$ ) are the dominant neutralizing agents at both sites, with higher NFs at RWESCK-KNUST. This corroborates the strong influence of dust and crustal materials, likely a conglomerate of Harmattan and construction. Ammonium ( $\text{NH}_4^+$ ), which is indicative of agricultural and organic sources, also contributes significantly to neutralization, particularly at RWESCK-KNUST, reflecting urban activities such as waste burning. Sodium ( $\text{Na}^+$ ) and potassium ( $\text{K}^+$ ) show lower NFs.

Comparatively, Sokoban is more influenced by biomass burning and industrial activities, while RWESCK-KNUST reflects a mix of crustal dust and anthropogenic emissions, particularly from vehicular sources.

The 72-hour back trajectory simulation ending on 20th February 2024 (Fig. 8a) reveals air mass origins that contributed to the atmospheric composition in Kumasi. The trajectories show that air masses originated from the northern part of the Gulf of Guinea and southern Ghana before reaching the study site. This suggests a strong maritime influence, with the air mass potentially carrying sea salt aerosols, which is reflected in the chloride ( $\text{Cl}^-$ ) concentrations in rainwater samples. Additionally, the vertical profile indicates that the air mass remained relatively low, fluctuating between 500 and 1500 m above ground level (AGL), which enhances the likelihood of the air mass interacting with local pollution sources. The mixture of marine and continental influences during this period aligns with the chemical signatures observed, particularly the presence of crustal elements such as calcium ( $\text{Ca}^{2+}$ ) and marine elements such as  $\text{Cl}^-$ .

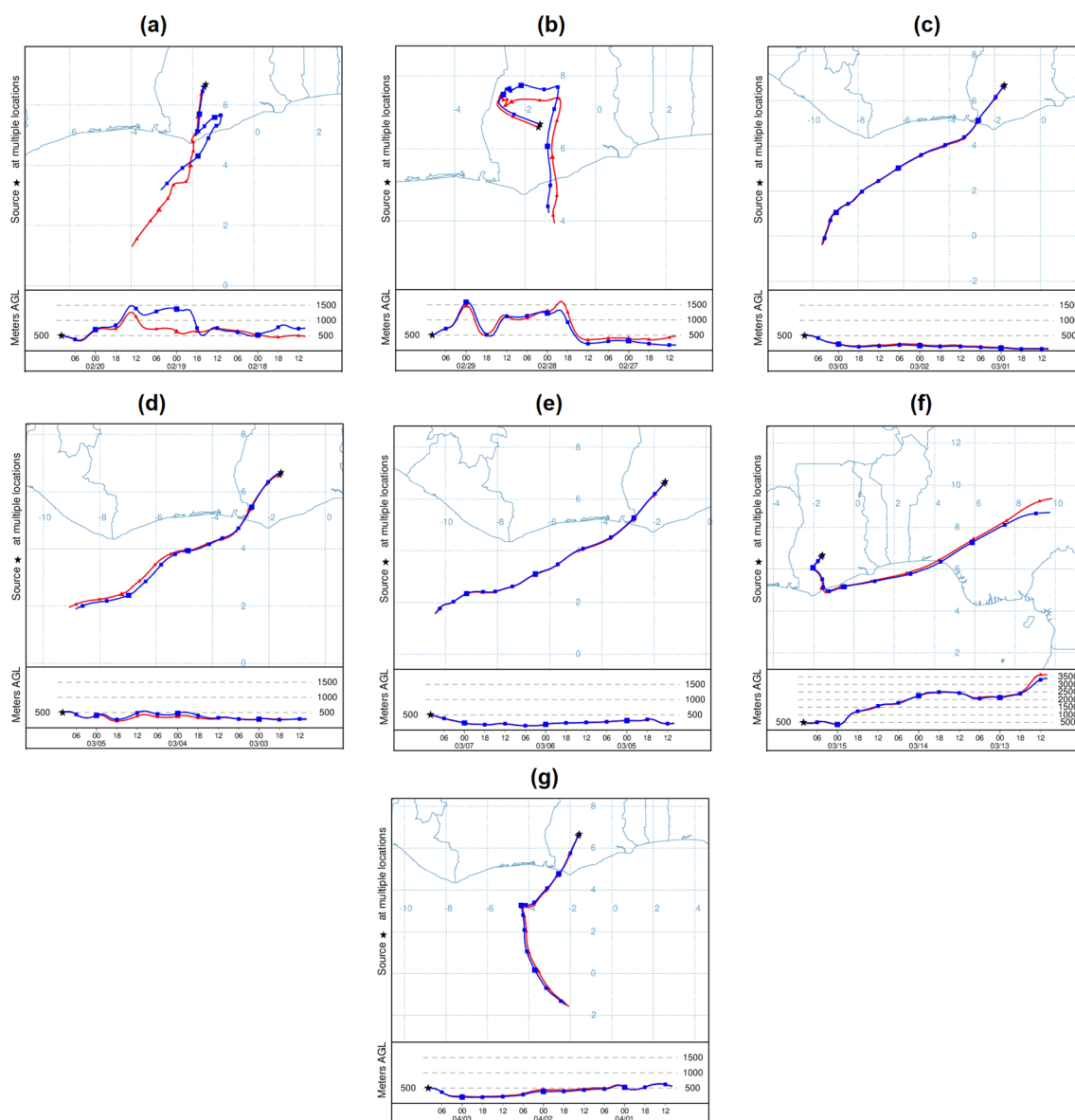


Fig. 8 The 72-h back trajectory during the (a) 3rd week of February 2024, (b) 4th week of February 2024, (c–e) 3rd, 5th, and 7th days of the 1st week of March 2024, (f) 2nd week of March 2024, and (g) 1st week of April 2024.



During the last week of February 2024 (Fig. 8b), air masses originated from southern regions, with an inland loop over the Gulf of Guinea before returning to the site. The looping pattern suggests prolonged atmospheric residence over the ocean. The air masses stayed relatively low, between 500 and 1500 m AGL. By the first week of March (3rd to 5th) 2024 (Fig. 8c–e) the air masses traveled from the southern Atlantic Ocean, moving northward across the Gulf of Guinea before reaching the study site. The trajectory remained relatively stable, with altitudes below 1500 m AGL, which suggests that the air masses primarily passed through marine and coastal environments. This trajectory supports the introduction of marine aerosols, particularly  $\text{Na}^+$  and  $\text{Cl}^-$ , with limited interaction with inland sources. The consistent low altitude indicates minimal mixing with higher atmospheric layers, allowing for significant contributions from marine aerosols, which is reflected in the chemical composition of the rainwater samples collected during this period.

During the second week of March 2024, particularly on 15th March 2024 (Fig. 8f), the air masses originated from the eastern region, traveling from the Sahelian areas of West Africa across northern Nigeria and Benin before reaching the study site. These air masses ascended to altitudes above 2000 m AGL, indicating potential long-range transport of dust and crustal materials from arid regions. The high altitude and extensive overland trajectory support the introduction of mineral dust and crustal ions (e.g.,  $\text{Ca}^{2+}$  and  $\text{Mg}^{2+}$ ). 72 hours before 3rd April 2024 (Fig. 8g), the air masses were moving from the south, originating over the Gulf of Guinea, and ascending gradually as they move inland toward the study site. The trajectory suggests a marine influence, likely contributing to increased concentrations of marine ions such as  $\text{Na}^+$  and  $\text{Cl}^-$  in the rainwater samples.

## 4. Conclusion

Pre-monsoon rainwater chemistry at Kumasi was used to assess the influence of atmospheric pollution and natural sources on the ionic composition. Both sites (Sokoban and RWESCK-KNUST) displayed elevated concentrations of nitrate ( $\text{NO}_3^-$ ) and ammonium ( $\text{NH}_4^+$ ), reflective of anthropogenic sources. Crustal ions such as calcium ( $\text{Ca}^{2+}$ ) and magnesium ( $\text{Mg}^{2+}$ ) were also present, with their levels largely influenced by the Harmattan dust and local emissions. The meteorological parameters played a critical role in modulating the ionic composition of rainwater. Rainfall, temperature, and wind speed were significant drivers, with rainfall acting as a scavenger of atmospheric pollutants. Temperature, particularly maximum temperature, promoted evaporation, hence concentrating ions in rainwater. Wind speeds largely influenced the resuspension of dust particles, contributing to elevated levels of crustal ions in rainwater samples. The enrichment factor (EF) analysis highlighted that both marine and crustal sources influenced the chemical composition of rainwater, with potassium ( $\text{K}^+$ ) showing strong enrichment from biomass burning, while nitrate ( $\text{NO}_3^-$ ) reflected anthropogenic pollution. Neutralization factors (NFs) demonstrated that calcium ( $\text{Ca}^{2+}$ ) and magnesium ( $\text{Mg}^{2+}$ ) were the dominant neutralizing agents,

mitigating the acidification of rainwater, especially at RWESCK-KNUST. The 72-hour back trajectory analysis further confirmed the interplay between local and regional air masses in shaping rainwater chemistry. Marine air masses contributed to sea salt aerosols, while long-range transport from the Sahel introduced dust and crustal materials. This mix of influences underscores the complexity of air quality management in Kumasi, where both natural and anthropogenic sources converge. Rainwater chemistry provides valuable insights into the sources and dynamics of atmospheric pollution, and the evaluation of the meteorological drivers and source contributions offers a practical approach for monitoring air quality. However, the limited sample size, dictated by the challenges of collecting adequate rainfall during the dry pre-monsoon season, highlights the need for future research with larger datasets spanning multiple seasons. Continuous sampling throughout the year, particularly capturing the early rainfall events, will enhance the robustness and generalizability of the findings. Future work should incorporate trace metal, organic, and isotopic analyses to improve source apportionment and offer more detailed chemical characterization of atmospheric deposition in tropical urban environments.

## Conflicts of interest

The authors declare no competing interests.

## Data availability

The back trajectory simulations for specific sampling days were undertaken using the Hybrid Single-Particle Lagrangian Integrated Trajectory (HYSPPLIT) model available at the NOAA Air Resources Laboratory (<https://www.ready.noaa.gov/hypub-bin/trajtype.pl>). The daily NASA-POWER meteorological data are available at <https://power.larc.nasa.gov/data-access-viewer/>. All resulting computational and statistical datasets used and/or analyzed during the current study are available from the corresponding author on reasonable request.

## Acknowledgements

We are thankful for the NASA POWER meteorological dataset obtained from the NASA Langley Research Center POWER Project funded through the NASA Earth Science Directorate Applied Science Program.

## References

- 1 J. Zeng, G. Han, S. Zhang, X. Xiao, Y. Li, X. Gao and R. Qu, Rainwater chemical evolution driven by extreme rainfall in megacity: Implication for the urban air pollution source identification, *J. Clean. Prod.*, 2022, **372**, 133732.
- 2 Á. Keresztesi, I. A. Nita, M. V. Birsan, Z. Bodor, T. Pernyeszi, M. M. Micheu and R. Szép, Assessing the variations in the chemical composition of rainwater and air masses using the zonal and meridional index, *Atmos. Res.*, 2020, **237**, 104846.



- 3 K. D. E. Journet, J. L. Rajot, S. Chevaillier, S. Triquet, P. Formenti and A. Zakou, Chemistry of rain events in West Africa: evidence of dust and biogenic influence in convective systems, *Appl. Cardiopulm. Pathophysiol.*, 2010, **10**, 9283–9293.
- 4 K. A. Koehler, S. M. Kreidenweis, P. J. DeMott, M. D. Petters, A. J. Prenni and C. M. Carrico, Hygroscopicity and cloud droplet activation of mineral dust aerosol, *Geophys. Res. Lett.*, 2009, **36**, L08805.
- 5 M. Ullah, M. S. Islam, F. Akter, M. Shohel, M. Rokonujjaman and A. Salam, Chemical composition and source apportionment of rainwater over Bangladesh during the monsoon, *Int. J. Environ. Sci. Technol.*, 2023, **20**(8), 8445–8456.
- 6 H. W. Xiao, H. Y. Xiao, A. M. Long, Y. L. Wang and C. Q. Liu, Chemical composition and source apportionment of rainwater at Guiyang, SW China, *J. Atmos. Chem.*, 2013, **70**(3), 269–281.
- 7 Á. Rostási, B. A. Topa, F. Gresina, T. G. Weiszburg, A. Gelencsér and G. Varga, Saharan dust deposition in central Europe in 2016—A representative year of the increased North African Dust removal over the last decade, *Front. Earth Sci.*, 2022, **10**, 869902.
- 8 K. Desboeufs, F. Fu, M. Bressac, A. Tovar-Sánchez, S. Triquet, J. F. Doussin and C. Guieu, Wet deposition in the remote western and central Mediterranean as a source of trace metals to surface seawater, *Atmos. Chem. Phys.*, 2022, **22**(4), 2309–2332.
- 9 A. R. H. de la Cruz, M. F. D. S. Pedreira, J. M. Godoy, P. Artaxo and A. Gioda, Chemical characterization and source apportionment of rainwater in Cuieiras Biological Reserve, central Amazon, Brazil, *Acta Amazonica*, 2024, **54**(3), e54es23131.
- 10 M. A. Aswini, S. Tiwari, U. Singh, S. Kurian, A. Patel, S. S. Gunthe and A. Kumar, Aeolian dust and sea salt in marine aerosols over the Arabian Sea during the southwest monsoon: Sources and spatial variability, *ACS Earth Space Chem.*, 2022, **6**(4), 1044–1058.
- 11 B. Ge, D. Xu, O. Wild, X. Yao, J. Wang, X. Chen and Z. Wang, Inter-annual variations of wet deposition in Beijing from 2014–2017: implications of below-cloud scavenging of inorganic aerosols, *ACP*, 2021, **21**, 9441–9454.
- 12 S. Sun, S. Liu, L. Li and W. Zhao, Components, acidification characteristics, and sources of atmospheric precipitation in Beijing from 1997 to 2020, *Atmos. Environ.*, 2021, **266**, 118707.
- 13 J. Zeng and G. Han, Rainwater chemistry reveals air pollution in a karst forest: Temporal variations, source apportionment, and implications for the forest, *Atmosphere*, 2020, **11**, 1315.
- 14 J. P. Weinstein, S. R. Hedges and S. Kimbrough, Characterization and aerosol mass balance of PM<sub>2.5</sub> and PM<sub>10</sub> collected in Conakry, Guinea during the 2004 Harmattan period, *Chemosphere*, 2010, **78**, 980–988.
- 15 V. Yoboué, C. Galy-Lacaux, J. P. Lacaux and S. Silué, Rainwater chemistry and wet deposition over the Wet Savanna Ecosystem of Lamto (Cote d'Ivoire), *J. Atmos. Chem.*, 2005, **52**, 117–141.
- 16 C. Galy-Lacaux and A. I. Modi, Precipitation chemistry in the Sahelian savanna of Niger, Africa, *J. Atmos. Chem.*, 1998, **30**, 319–343.
- 17 W. Li, Y. Zhou, W. Zhang, D. Liu, T. Hu, F. Wu and D. Zhang, A Review of Water-Soluble Ions in Natural Dust Particles Over East Asia: Abundance, Spatial Distributions, and Implications, *ACS ES&T Air*, 2025, **2**(8), 1379–1393.
- 18 J. F. Kok, T. Storelvmo, V. A. Karydis, A. A. Adebisi, N. M. Mahowald, A. T. Evan and D. M. Leung, Mineral dust aerosol impacts on global climate and climate change, *Nat. Rev. Earth Environ.*, 2023, **4**(2), 71–86.
- 19 D. S. Bisht, S. Tiwari, A. K. Srivastava, J. V. Singh, B. P. Singh and M. K. Srivastava, High concentration of acidic species in rainwater at Varanasi in the Indo-Gangetic Plains, India, *Nat. Hazards*, 2015, **75**(3), 2985–3003.
- 20 S. N. Narh, S. A. Takyi, M. O. Asibey and O. Amponsah, Garden city without parks: an assessment of the availability and conditions of parks in Kumasi, *Urban For. Urban Green.*, 2020, **55**, 126819.
- 21 C. Mensah, J. Atayi, A. T. Kabo-Bah, M. Švik, D. Acheampong, R. Kyere-Boateng and M. V. Marek, Impact of urban land cover change on the garden city status and land surface temperature of Kumasi, *Cogent Environ. Sci.*, 2020, **6**, 1787738.
- 22 J. Agyekum, L. K. Amekudzi, T. Stein, J. N. Aryee, W. A. Atiah, E. A. Adefisan and S. K. Danuor, Verification of satellite and model products against a dense rain gauge network for a severe flooding event in Kumasi, Ghana, *Meteorol. Appl.*, 2023, **30**, e2150.
- 23 B. F. Frimpong, A. Koranteng and F. Molkenthin, Analysis of temperature variability utilising Mann–Kendall and Sen's slope estimator tests in the Accra and Kumasi Metropolises in Ghana, *Environ. Syst. Res.*, 2022, **11**, 24.
- 24 M. A. Osei, M. Padi, B. Yahaya, M. Baidu, E. Quansah, J. N. Aryee and L. K. Amekudzi, The dynamics of dry and wet monsoon MCS formation over West Africa: Case assessment of February 13, 2018 and June 18, 2018, *Q. J. Roy. Meteorol. Soc.*, 2023, **149**, 133–151.
- 25 J. N. Aryee, L. K. Amekudzi and E. I. Yamba, Low-Level Cloud Development and Diurnal Cycle in Southern West Africa During the DACCIWA Field Campaign: Case Study of Kumasi Supersite, Ghana, *J. Geophys. Res. Atmos.*, 2021, **126**, e2020JD034028.
- 26 WMO, *Manual for the GAW precipitation chemistry programme: guidelines, data quality objectives and standard operating procedures*, 2004.
- 27 J. N. Pereira, A. Fornaro and M. Vieira-Filho, Atmospheric deposition chemistry in a Brazilian rural area: alkaline species behavior and agricultural inputs, *Environ. Sci. Pollut. Res. Int.*, 2021, **28**, 23448–23458.
- 28 D. Majumdar and H. Adhikary, Identification of sources of ions in early monsoon precipitation over Kolkata Metropolis and two adjoining towns, *Urban Clim.*, 2022, **41**, 101087.



- 29 P. J. Asilevi, F. Dogbey, P. Boakye, J. N. A. Aryee, E. I. Yamba, S. Y. Owusu, L. K. Amekudzi, *et al*, Bias-corrected NASA data for aridity index estimation over tropical climates in Ghana, West Africa, *J. Hydrol. Reg. Stud.*, 2024, **51**, 101610.
- 30 P. Asilevi Junior, N. K. Opoku, F. Martey, E. Setsoafia, F. Ahafianyo, E. Quansah, M. Padi, *et al.*, Development of High Resolution Cloud Cover Climatology Databank Using Merged Manual and Satellite Datasets over Ghana, West Africa, *Atmos.-Ocean*, 2022, **60**, 566–579.
- 31 P. A. Junior, E. Quansah and F. Dogbey, Satellite-based estimates of photosynthetically active radiation for tropical ecosystems in Ghana—West Africa, *Trop. Ecol.*, 2022, **63**, 615–625.
- 32 A. D. Quansah, F. Dogbey, P. J. Asilevi, P. Boakye, L. Darkwah, S. Oduro-Kwarteng and P. Mensah, Assessment of solar radiation resource from the NASA-POWER reanalysis products for tropical climates in Ghana towards clean energy application, *Sci. Rep.*, 2022, **12**, 10684.
- 33 L. C. Guo, Y. Zhang, H. Lin, W. Zeng, T. Liu, J. Xiao and W. Ma, The washout effects of rainfall on atmospheric particulate pollution in two Chinese cities, *Environ. Pollut.*, 2016, **215**, 195–202.
- 34 M. Zdeb, D. Papciak and J. Zamorska, An assessment of the quality and use of rainwater as the basis for sustainable water management in suburban areas, *E3S Web Conf.*, 2018, **45**, 0011.
- 35 V. A. Edlabadkar, R. U. Soni, A. B. M. S. Doulah, S. Y. Owusu, S. Hackett, J. M. Bartels, N. Leventis and C. Sotiriou-Leventis, CO<sub>2</sub> Uptake by Microporous Carbon Aerogels Derived from Polybenzoxazine and Analogous All-Nitrogen Polybenzodiazine Aerogels, *Chem. Mater.*, 2024, **3**, 1172–1187.
- 36 R. Kumar, R. Kumar, A. Singh, *et al.*, Chemometric approach to evaluate the chemical behavior of rainwater at high altitude in Shaune Garang catchment, Western Himalaya, *Sci. Rep.*, 2022, **12**, 12774.
- 37 D. Majumdar and H. Adhikary, Identification of sources of ions in early monsoon precipitation over Kolkata Metropolis and two adjoining towns, *Urban Climate*, 2022, **41**, 101087.
- 38 C. E. Junge and R. T. Werby, The Concentration of Chloride, Sodium, Potassium, Calcium and Sulfate in Rain Water over the United States, *J. Meteorol.*, 1958, **15**, 417–425.
- 39 H. Wang and Q. Zhang, Research Advances in Identifying Sulfate Contamination Sources of Water Environment by Using Stable Isotopes, *Int. J. Environ. Res. Publ. Health*, 2019, **16**, 1914.

